Polym Int 53:1693–1703 (2004)
DOI: 10.1002/pi.1530

Thermoplastic elastomers from rubber and recycled polyethylene: chemical reactions at interphases for property enhancement

Olga Grigoryeva,[1] Alexander Fainleib,[1] Olga Starostenko,[1] Alexander Tolstov[1] and Witold Brostow[2,3]*

[1] Institute of Macromolecular Chemistry of the National Academy of Sciences of Ukraine, 48 Harkivske shose, 02160 Kyiv, Ukraine
[2] Department of Materials Science and Engineering, University of North Texas, PO Box 305310, Denton, TX 76203-5, USA
[3] Center for Applied Physics and Advanced Technology (CFTA), National University of Mexico, Queretaro, Mexico

Abstract: Recycled low density polyethylene (R-LDPE) has been reactively compatibilized with butadiene rubber (BR) by using small additions of reactive polyethylene copolymers and reactive BRs to produce thermoplastic elastomers (TPEs). TPEs were characterized by thermogravimetric analysis (TGA), differential scanning calorimetry (DSC), dynamic mechanical analysis (DMA), rheology measurements, wide-angle X-ray scattering (WAXS) and mechanical testing. WAXS results show that the presence of BR and reactive modifiers does not completely prevent the crystallization of R-LDPE during the TPE formation. Depression of the melting point has been found in all cases. Also in all cases, compatibility is provided by formation of interfacial layers. The best mechanical characteristics are obtained for R-LDPE + BR blends compatibilized with poly(ethylene-*co*-acrylic acid) (PE-*co*-AA) and polybutadiene terminated with isocyanate groups (PB-NCO) for PB-NCO = 7.5 wt% per PB and COOH/NCO ratio = 1/1. The stress at break and elongation at break are respectively improved by 31 % and 63 %. The PB-NCO modifier participates in co-vulcanization with BR in the rubber phase and reacts at the interface with the PE-*co*-AA dissolved in the polyolefin phase. As a result, the amorphous phase of R-LDPE is dissolved by the rubber phase and a morphology with dual phase continuity is formed, assuring an improvement of mechanical properties of TPEs.

Keywords: recycling; dynamic vulcanization; reactive compatibilization; LDPE; BR; TPE

INTRODUCTION

It is known that thermoplastic elastomers (TPEs) can be produced from polymer blends consisting of non-vulcanized virgin rubber and thermoplastic polymers such as polyolefins.[1–9] The TPE properties can be much improved by a dynamic or *in situ* curing.[2–5,7,9] During dynamic vulcanization, carried out by intense mixing above the melt temperature of the thermoplastic polymer, the rubber phase will be crosslinked (vulcanized) and finely dispersed (mean particle size of a few microns) in the thermoplastic. The latter takes the role of the matrix.[4] The resulting TPE exhibits rubbery characteristics while maintaining the thermoplasticity of the matrix. As a consequence, the TPE is melt (re)processable. A further benefit of TPEs is that they provide high value-added products if the components are derived from waste sources ('upcycling'). Preliminary results show that the TPEs can be adopted for certain post-consumer goods.[10–12] Since thermoplastic and rubber are usually incompatible, providing component compatibility via an enhancement of interfacial adhesion is needed.[13–16]

The reactive compatibilization can be realized by several ways.[13,15] In this work, we introduce reactive polyethylene copolymer into a thermoplastic phase and reactive polybutadiene rubber into a rubber phase.[17,18] The functional groups of polymer additives used should be reactive with each other. During intensive mixing of components at an elevated temperature a chemical reaction occurs at the interface, leading to increased adhesion between thermoplastic and rubber phases. The morphology of such compatibilized TPEs should result in a reinforcement of their mechanical properties.

EXPERIMENTAL

Materials

The virgin butadiene rubber (BR) (weight-average molecular weight $M_w = 21\,000\,g\,mol^{-1}$ was SKD-2

* Correspondence to: Prof Witold Brostow, Department of Materials Science, University of North Texas, Denton, TX 76203-5310, USA
E-mail: brostow@unt.edu
Contract/grant sponsor: European Union INCO-Copernicus project; contract/grant number: ICA2-CT-2001-10003
Contract/grant sponsor: US Department of Commerce, Washington, DC (SABIT Program)
(*Received 19 July 2003; revised version received 4 September 2003; accepted 10 October 2003*)
Published online 30 July 2004

 Polym Int 0959–8103/2004/$30.00

from Voronezhsintezkauchuk, Voronezh, Russia. Its Mooney viscosity *ML* (1 + 4) at 130 °C is 46. Recycled low density polyethylene (R-LDPE) was made from greenhouse films containing 65–70 % LDPE, 12–17 % linear LDPE, 12–15 % poly(ethylene-*co*-vinyl acetate), additives (kaolin, talc, silica, short-term antioxidant for processing, long-term antioxidant for stability) ≈500 ppm, UV stabilizers (amine, benzophenone) ≈2500 ppm. The melt flow index (*MFI*) values are: $MFI_{190/2.16} = 0.29$ g/10 min and $MFI_{230/2.16} = 0.95$ g/10 min. Post-consumer greenhouse films were collected in the province of Ragusa (Sicily, Italy) after nearly one year of exploitation, and were washed, dried and cut to pieces by an industrial-scale machine.

As a standard sample, a virgin LDPE (V-LDPE), Riblene FC30 from Polimeri Europe, Rome, Italy, was used. This polymer is used for greenhouse film applications and has the following characteristics: number-average molecular weight) $M_n = 31\,100$ g mol^{-1}, $M_w = 179\,200$ g mol^{-1}, $M_z = 487\,200$ g mol^{-1}, $M_w/M_n = 5.76$, $M_z/M_w = 2.72$; the melt flow index values are: $MFI_{190/2.16} = 0.28$ g/10 min and $MFI_{230/2.16} = 0.8$ g/10 min.

Reactive compatibilization and TPE preparation

The reactive thermoplastics and reactive rubbers used are defined in Table 1. All polyethylene copolymers and polybutadienes terminated with epoxy, amine and carboxyl groups were from Aldrich Chemicals. Polybutadiene with terminal isocyanate groups was Krasol LBD from Kaucuk, a.s.—Unipetrol Group, Prague, Czech Republic. Materials were used as received. The compositions used are listed in Table 2.

Polymers were mixed in a twin-rotor mixer of the Brabender type at 180 °C at 100 rpm for 10 min. In all cases, BR with reactive polybutadiene rubber, ZnO and stearic acid were mixed first for 2 min before the addition of LDPE with a reactive polyethylene copolymer. For dynamic vulcanization, curing agents were added after 2 min of mixing BR with molten LDPE and mixed for a further 6 min. We relied on results of torsion torque *vs* time determination which gave us 10 min as the time of the maximum value of torsion torque. The TPE sheets with thickness of 1 mm were produced by compression molding at 180 °C under a pressure of 10 MPa.

Table 1. Reactive thermoplastics and reactive rubbers used

Name	Code	Content of reactive groups (wt%)
Reactive thermoplastics:		
Poly(ethylene-*co*-acrylic acid)	PE-*co*-AA	5.0
Poly(ethylene-*co*-glycidyl methacrylate)	PE-*co*-GMA	8.0
Poly(ethylene-*co*-vinyl acetate-*co*-acrylic acid)	PE-*co*-VA-*co*-AA	1.0
Poly(ethylene-*graft*-maleic anhydride)	PE-*g*-MAH	3.0
Reactive rubbers:		
Polybutadiene, terminated with epoxy groups	PB-E	16.0
Polybutadiene, terminated with amine groups	PB-NH_2	1.2
Polybutadiene, terminated with carboxyl groups	PB-COOH	1.9
Polybutadiene, terminated with isocyanate groups	PB-NCO	2.6

Table 2. Compositions

Additives[a]	Component content (wt%)
Recycled R-LDPE	60
Butadiene rubber, BR	40
Stearic acid	1
Sulfur	3
Bis-(2-benzothiazolyl)disulfide	1
Zinc oxide	5
Reactive couples:	
Reactive rubbers	1.5:15.0
Reactive thermoplastics	Variable[b]

[a] All additive (excluding R-LDPE) concentrations are with respect to BR.
[b] The stoichiometric ratio of functional groups of reactive rubbers and thermoplastics = 1:1 for all compositions.

Characterization techniques

Thermogravimetric analysis (TGA) was performed using the Q-1500D Derivatograph system developed by F Paulik, J Paulik and L Erdey from Magyar Optikai Muvek Vevoszolgalat, Budapest, Hungary. We investigated the temperature range from 290 to 875 K at a heating rate 10 K min^{-1} in air with evacuation of gaseous products of degradation. The sample weight was around 50 mg.

Wide-angle X-ray scattering (WAXS) curves were recorded with an X-ray DRON-4-07 diffractometer from Orelnauchpribor, Orel, Russia, using Cu-K_α radiation monochromatized by a Ni filter. The mean size of the crystallites $\langle D \rangle$ was calculated using the Scherer equation,[19] the crystal lattice spacing $\langle d \rangle$ (ie the distance between reflecting planes) was calculated from the Bragg equation,[19] and the degree of crystallinity $\langle X \rangle$ was calculated using the Matthews method.[20]

Differential scanning calorimetry (DSC) thermograms were obtained using a calorimeter with diathermic cells under nitrogen in the temperature range from 293 to 413 K and a heating rate of 2 K min^{-1}. The sample weight was 15–20 mg. The temperature dependence of heat capacity C_p was determined and the degree of crystallinity was calculated using the Lupolen standard from Hoechst AG, Frankfurt/Main, Germany, assumed to have 100 % crystallinity and the enthalpy of melting $H_m = 290$ J g^{-1}.

Rheological measurements were performed using an MV-2 capillary microviscosimeter of the melt indexer type[21] (the capillary diameter and length are respectively 1.26 and 8.3 mm) at temperatures of 413, 433, 453 and 473 K. The wall shear stress τ_w, wall

shear rate γ_w, and shear viscosity η were calculated using standard equations.[3]

Dynamic mechanical thermal analysis (DMA) measurements in the tensile mode were performed with a viscoelastometer of the Rheovibron type with temperature scans from 173 to 445 K at frequency 100 Hz and a heating rate of 2.0 K min^{-1}. Dimensions of samples were 5.0 cm × 0.5 cm × 0.1 cm. The temperature corresponding to the maximum of the loss modulus E'' was taken as the glass transition temperature T_g.[21]

In order to estimate the crosslinking degree of both LDPEs, the residual gel content was determined via Soxhlet extraction using *o*-xylene. The extraction was carried out for 8 h (≈10 times circulation of solvent per hour) followed by drying the samples in an air oven (50 °C for 24 h) prior to weighing. The *o*-xylene insoluble fraction was considered to correspond to the residual gel content.

Mechanical testing was performed with an Instron 1122 machine at the ambient temperature at the elongation rate (the speed of upper cross-arm) 50 mm min^{-1}; averages for 6–7 specimens were calculated to obtain the stress at break σ_b and the elongation at break ε_b.

COMPARISON OF VIRGIN AND RECYCLED LDPEs

V-LDPE and R-LDPE thermooxidative degradation in air was determined. The respective differential thermal analysis (DTA), differential thermogravimetry (DTG) and thermogravimetry (TG) curves are shown in Fig 1 and also reported in Table 3. One can see that the curves for V-LDPE and R-LDPE are similar. The DTA curves (Fig 1(a)) show an endothermic peak, the result of melting V-LDPE and R-LDPE (at 393 K and 388 K, respectively), and a few low-resolved high temperature exothermic peaks due to oxidative destruction of the PEs since at those temperatures the antioxidants lose much of their effect. V-LDPE and R-LDPE have similar temperatures for the beginning of intensive degradation (near 600 K) and char residue values of 3.5 and 5 %, respectively (see Fig 1 (c) and Table 3). The appearance of an additional degradation stage (at 548–693 K in Fig 1(b)) and the high temperature shift of all TGA, DTG and TG curves, as well as the increasing melting temperature (see Fig 1(a)) and value of char residue (see Table 3) reflect the existence of thermally more stable structures in R-LDPE compared to V-LDPE. It is clear that partial degradation of R-LDPE chains and formation of branched or crosslinked chains takes place.

WAXS curves for V-LDPE and R-LDPE are shown in Fig 2(a). Both diffractograms contain two sharp peaks at the scattering angles of 21.1° and 23.4° (characteristic for orthorhombic crystal cell of polyethylene) identified as the (110) and (200) polyethylene strongest reflections, respectively.[22] The diffuse maximum located at 19.5° corresponds to R-LDPE amorphous phase.[23] Thus, we find no appreciable differences in crystal cell or amorphous phase periodicities since V-LDPE and R-LDPE have similar mean sizes of microcrystals $\langle D \rangle = 10.7$ and 11.1 nm, respectively, and identical crystal lattice spacing $\langle d \rangle = 0.421$ nm. The results are summarized in Table 4. However, it can be seen that V-LDPE has a higher degree of crystallinity $\langle X \rangle$ than R-LDPE. This can be explained by a reduction of molecular weight of R-LDPE due to additional thermooxidative destruction as well as crosslinking during the outdoor service and reprocessing. R-LDPE clearly has a higher content of the amorphous phase than V-LDPE. The BR studied is a typical amorphous polymer (see Fig 2(b)) and three sharp peaks in the range

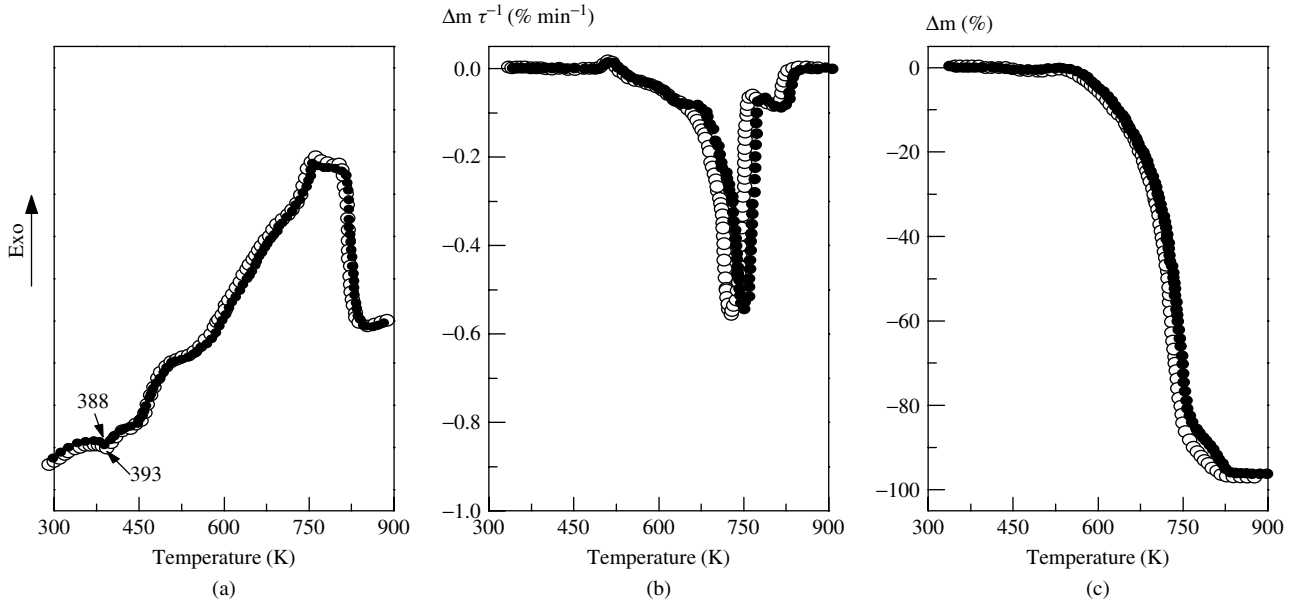

Figure 1. Thermogravimetric analysis curves for V-LDPE (open circle) and R-LDPE (solid circle): (a) differential thermal analysis (DTA); (b) differential thermogravimetry (DTG); (c) thermogravimetry (TG).

of approximately 32–36° can be attributed to low molecular weight additives used in the curing process (see Table 2).

The WAXS data agree with DSC results (Fig 3(a)). It is confirmed that the BR studied is amorphous. Two relaxations at 203–249 K and 319–383 K are evidence of some heterogeneity of the BR structure. The first transition has to be assigned to the α-relaxation process, ie the glass transition temperature T_g of flexible (uncrosslinked) BR chains, $T_g = 226$ K. Note that the value of the heat capacity jump ΔC_p at the T_g is small, namely $\Delta C_p = 0.1\,J\,g^{-1}\,K^{-1}$. Thus, the number of segments of BR chains not limited by crosslinking bonds (uncured molecules) is not significant. The second high temperature transition reflects the mobility of BR segments limited by intermolecular crosslinking (cured structure); the higher value of $\Delta C_p = 0.24\,J\,g^{-1}\,K^{-1}$ is evidence of a considerable proportion of such segments.

The C_p (T) plots of both LDPEs are shown in Fig 3. One can see that both V-LDPE and R-LDPE have typical curves for semicrystalline polyolefins with a 'solid–liquid' phase transition at 310–391 K and 322–389 K, respectively. These values and the

Table 3. Thermal behavior of V-LDPE and R-LDPE

Sample studied	Char residue (%)	Interval of weight loss (T_{onset}/T_{end}) (K)	T_{max} rate (K)	Weight loss (%)
V-LDPE	3.5			
		463/498	478	−2
		503/573	553	2
		673/773	743	70
		753/833	803	91
R-LDPE	5			
		463/498	483	−2
		498/568	533	2
		548/693	633	10
		683/773	748	75
		773/833	813	95

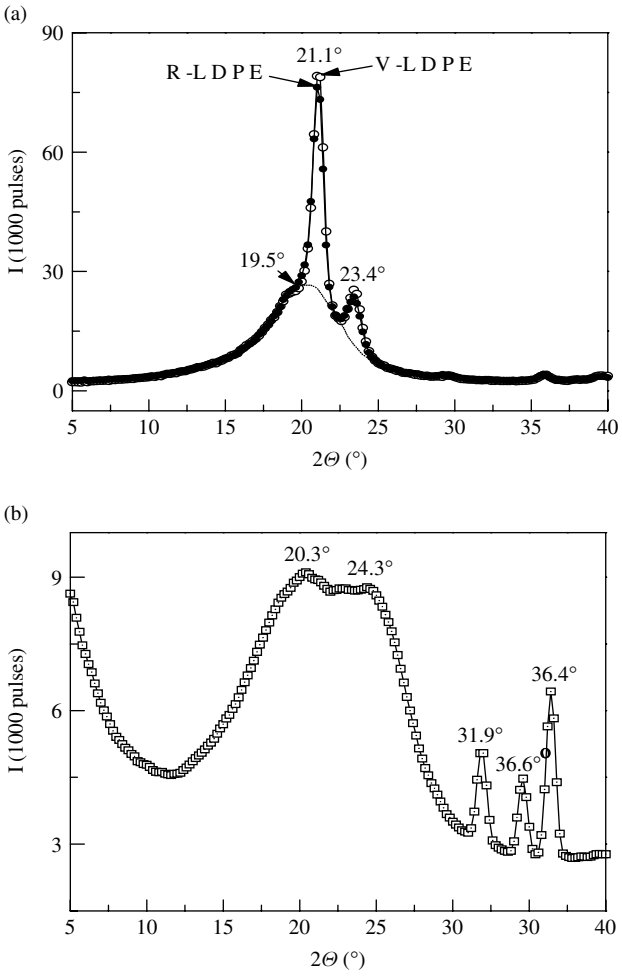

Figure 2. WAXS curves for: (a) V-LDPE (open circle) and R-LDPE (solid circle); (b) BR cured.

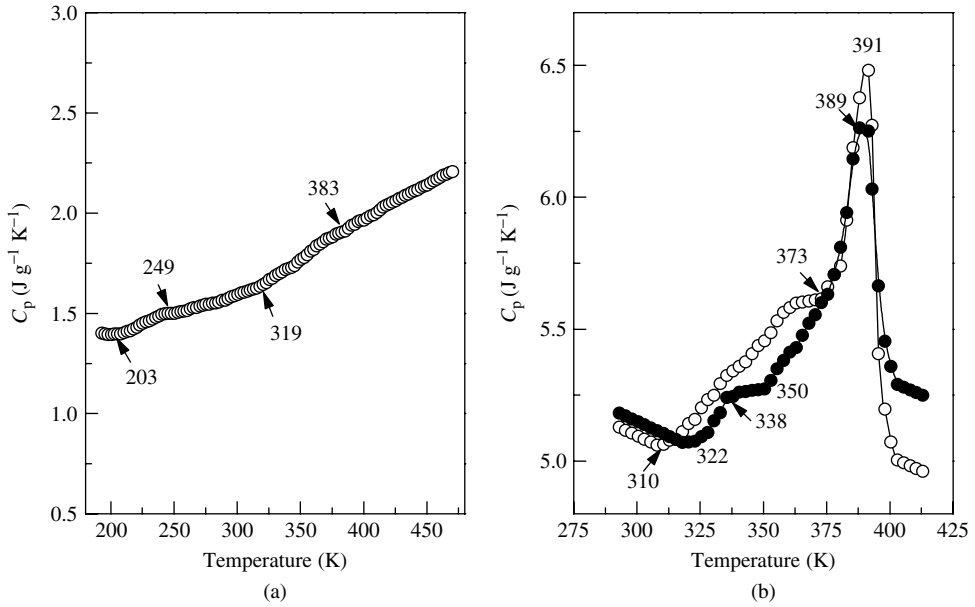

Figure 3. Temperature dependence of specific heat capacity C_p of: (a) cured BR; (b) V-LDPE (open circle) and R-LDPE (solid circle).

melting peak temperature, $T_m = 389$ K, for R-LDPE are quite similar to the values reported for other post-consumer LDPEs.[24] In contrast to V-LDPE, the melting of the crystalline phase of R-LDPE consists of melting low molecular weight crystallites (probably with defects) at 322–338 K followed by melting high molecular weight crystallites at 389 K;[25] we note that R-LDPE contains some linear LDPE and ethylene-vinylacetate copolymer (EVA). We assume the shoulder at 338–350 K without any visible changes in the values of C_p reflects recrystallization of the low molecular weight crystallites of R-LDPE into high molecular weight ones. The common decrease of values of C_p between 322 and 373 K observed for R-LDPE in comparison with V-LDPE is evidence of increasing packing density of the former due to formation of branched or crosslinked polymer chains already mentioned. It can be seen that V-LDPE has a higher degree of crystallinity X than R-LDPE, supporting the WAXS results.

Tensile properties and residual gel content values for V-LDPE and R-LDPE samples are presented in Table 4. Increasing residual gel content value and some reduction in tensile properties observed for R-LDPE confirm the above conclusions.

Rheological behavior of V-LDPE and R-LDPE is presented graphically in Fig 4. One can see that for both V-LDPE and R-LDPE at each temperature studied the flow curves (Fig 4(a)) are very similar, including the values of viscosity. The shear rate dependence of melt viscosity (in Arrhenius coordinates) of both V-LDPE and R-LDPE is shown in Fig 4(b). Based on the data presented, the flow activation energies E_a were calculated and found to be practically the same for both polymers, $E_a \approx 47$ kJ mol^{-1}.

In summary, V-LDPE and R-LDPE have no significant differences in thermal, rheological and mechanical properties; therefore, R-LDPE can be used in TPE compositions with useful properties.

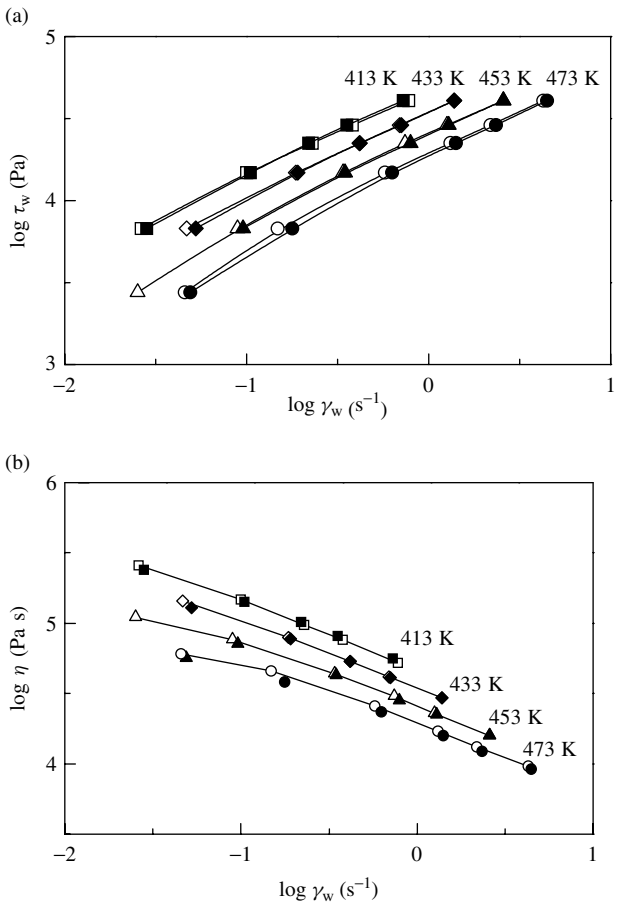

Figure 4. Dependence of (a) shear stress τ_w *versus* shear rate γ_w and (b) shear viscosity η *versus* shear rate for V-LDPE (open circle) and R-LDPE (solid circle) at several temperatures.

REACTIVE COMPATIBILIZATION OF R-LDPE + BR AND TPE FORMATION

As inferred above, we achieved reactive compatibilization by introduction of reactive polyethylene copolymer into the thermoplastic phase and reactive polybutadiene rubber into the rubber phase to enhance the interfacial adhesion by means of chemical interaction between the functional groups of compatibilizing agents at the thermoplastic/rubber interface. The reactions occur during melt mixing of components during TPE formation. The respective reaction schemes are shown in Fig 5. Thus, we have the following reactive couples of functional groups: epoxy + carboxyl (1 and 2), amine + epoxy (3), amine + anhydride (4), isocyanate + anhydride (5), isocyanate + epoxy (6) and isocyanate + carboxyl (7 and 8).

Tensile properties of TPEs determined for different reactive couples are displayed as block diagrams in Fig 6. The effect of compatibilization is observed for TPEs obtained by using the following reactive couples: PB-NH_2 + PE-*co*-GMA, PB-NCO + PE-*co*-AA and PB-NCO + PE-*co*-VA-*co*-AA. These reactive couples act as interfacial agents promoting adhesion between the matrix and the dispersed phase.

Table 4. Properties of V-LDPE and R-LDPE

Material	T_m (K)		Degree of crystallinity X (%)		Mean size of crystallites D (nm)	Crystal lattice spacing d (nm)	σ_b (Mpa)	ε_b (%)	Gel content[a] (wt%)
	DSC	DTA	DSC	WAXS					
V-LDPE	391	393	47	29.2	10.7	0.421	11.0	668	0
R-LDPE	389	388	43	27.5	11.1	0.421	7.1	440	6

[a] Determined as *o*-xylene insoluble fraction.

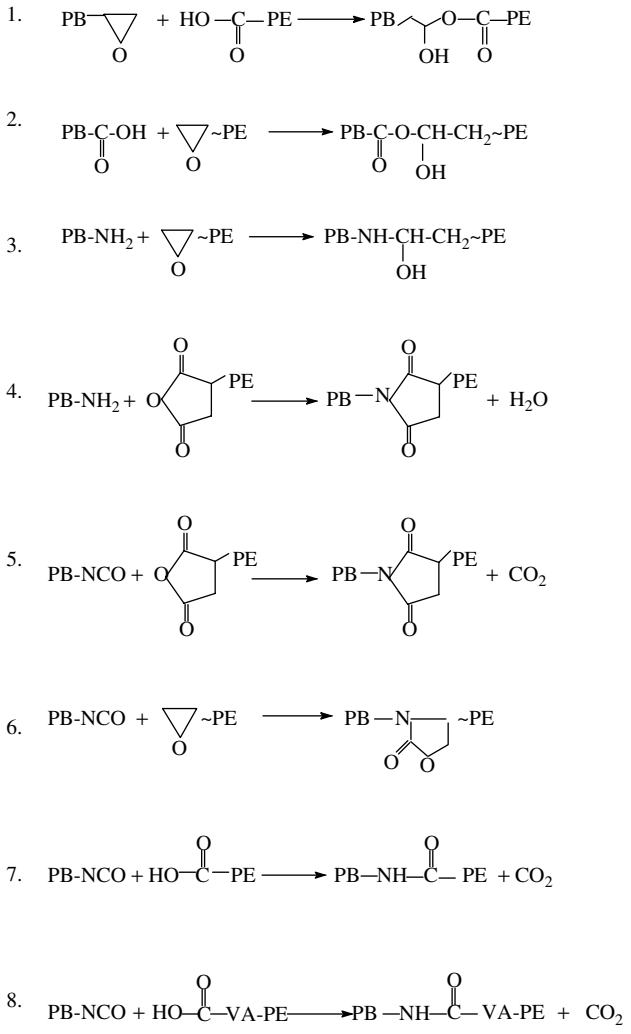

Figure 5. Reaction schemes between reactive polyethylenes and reactive butadiene rubbers: PB-E + PE-*co*-AA (1); PB-COOH + PE-*co*-GMA (2); PB-NH_2 + PE-*co*-GMA (3); PB-NH_2 + PE-*g*-MAH (4); PB-NCO + PE-*g*-MAH (5); PB-NCO + PE-*co*-GMA (6); PB-NCO + PE-*co*-AA (7); PB-NCO + PE-*co*-VA-*co*-AA (8).

The largest improvement in mechanical characteristics is seen for R-LDPE (PE-*co*-AA) + BR (PB-NCO) TPE: its values of σ_b and ε_b are higher by 31 and 63 %, respectively, than those for the unmodified R-LDPE + BR TPE. The reason for the difference is clearly the reaction between PE-*co*-AA and PB-NCO at the interface.

Our conclusion is confirmed by the results presented in Figs 7–9. Introduction of the PB-NCO + PE-*co*-AA (NCO/COOH = 1/1) compatibilizer enhances the tensile properties (Fig 7). We achieved maximal values at approximately 8–10 wt% of PB-NCO (per BR). However, a further increase of PB-NCO content up to 15 wt% lowers the elongation at break values. We infer that PB-NCO can also react with unsaturated bonds of the BR inside the rubber phase, as is evident from the gel content data presented in Fig 8. One can see an approximately linear (perhaps slightly concave) growth of the gel content value with increasing PB-NCO content in the BR phase.

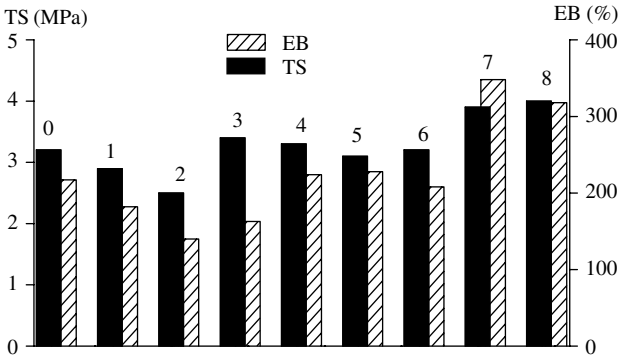

Figure 6. Tensile properties of unmodified R-LDPE/BR = 60/40 wt% TPE (0) and the same TPE modified by: PB-E + PE-*co*-AA (1); PB-COOH + PE-*co*-GMA (2); PB-NH_2 + PE-*co*-GMA (3); PB-NH_2 + PE-*g*-MAH (4); PB-NCO + PE-*g*-MAH (5); PB-NCO + PE-*co*-GMA (6); PB-NCO + PE-*co*-AA (7); PB-NCO + PE-*co*-VA-*co*-AA (8). All PB-modifiers were used in the amount of 7.5 wt% (per BR), and the ratio of functional groups for PB- and PE-based modifiers was kept at 1/1. The symbol TS is used in the figure for the stress at break σ_b; the symbol EB is used for the elongation at break ϵ_b.

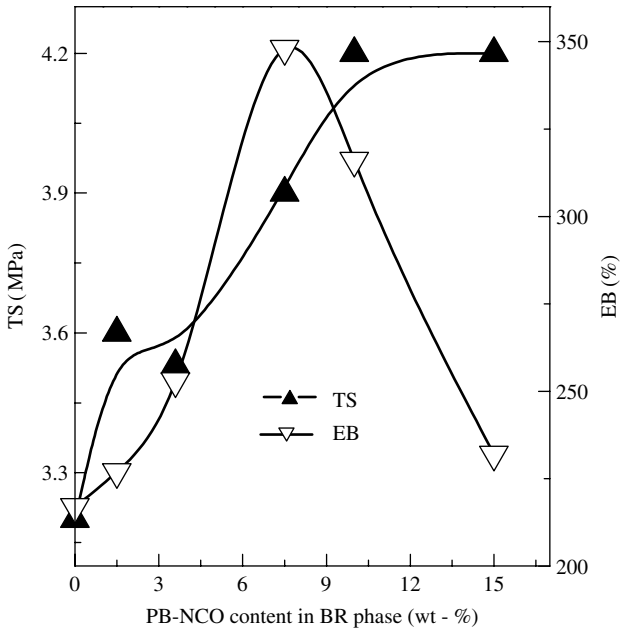

Figure 7. Tensile properties of R-LDPE (PE-*co*-AA) + BR (PB-NCO) TPEs *versus* PB-NCO content in BR phase with the NCO/COOH ratio equal to 1/1. The symbol TS is used in the figure for the stress at break σ_b; the symbol EB is used for the elongation at break ϵ_b.

As seen in Fig 9, the addition of PE-*co*-AA to PB-NCO increases the tensile properties of TPEs, reaching a plateau at NCO/COOH = 1/1. The excess of PE-co-AA (≥1.5 e.e.w. (equal equivalent weight ratio) per PB-NCO) does not influence the tensile properties significantly. We explain this by lower reactivity of COOH groups in comparison with NCO groups. Minimal values of σ_b and ε_b are observed for the TPEs modified by PB-NCO (7.5 wt% per BR) without any PE-*co*-AA. Clearly, in this case the interfacial adhesion between the TPE components is comparable to that in unmodified TPE. In addition, a decrease of ε_b value (by approximately 15 %)

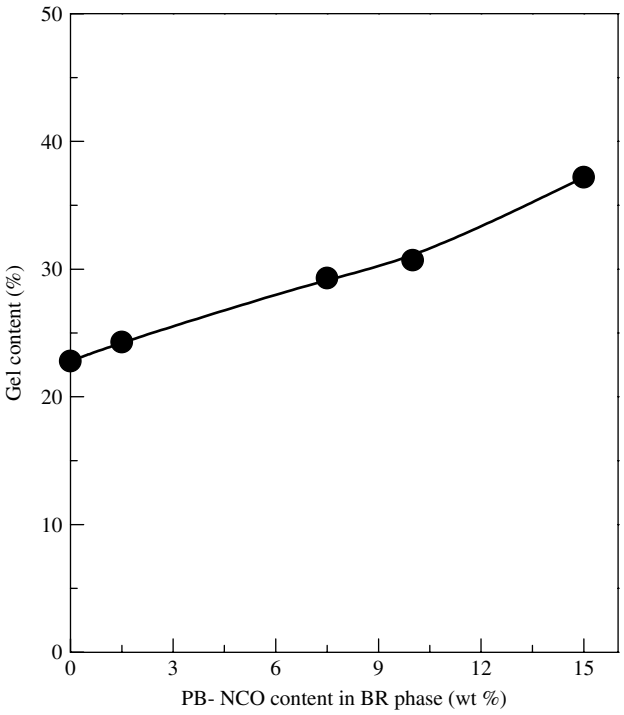

Figure 8. Gel content of TPEs *versus* PB-NCO content in the BR phase. R-LDPE/BR = 60/40 wt% for all TPEs and the ratio of functional groups for PB- and PE-based modifiers = 1/1.

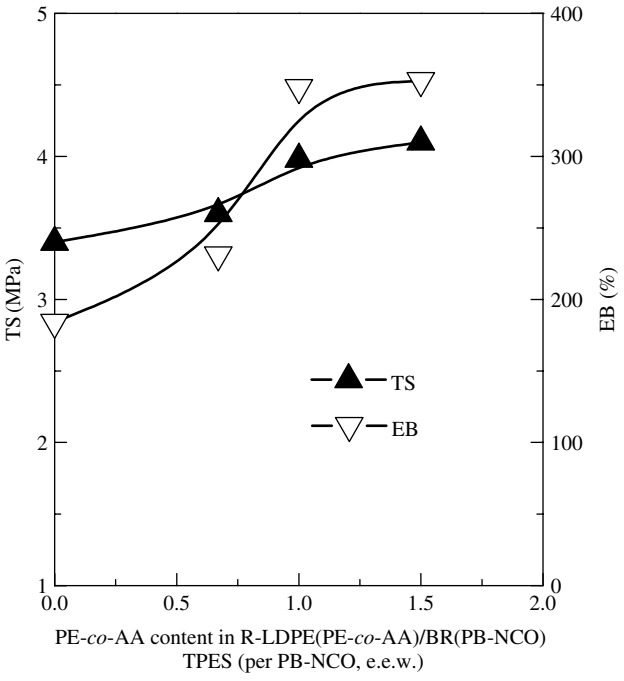

Figure 9. Tensile properties of R-LDPE (PE-*co*-AA) + BR (PB-NCO) TPEs *versus* PE-*co*-AA e.e.w. per PB-NCO (at 7.5 wt% PB-NCO content per BR). The symbol TS is used in the figure for the stress at break σ_b; the symbol EB is used for the elongation at break ϵ_b.

for this sample in comparison with unmodified R-LDPE + BR TPE shows that PB-NCO indeed reacts with unsaturated bonds of BR inside the rubber phase.

The absence of a compatibilizing effect for the other reactive couples used is probably related to kinetic/diffusion peculiarities. Apparently, for these

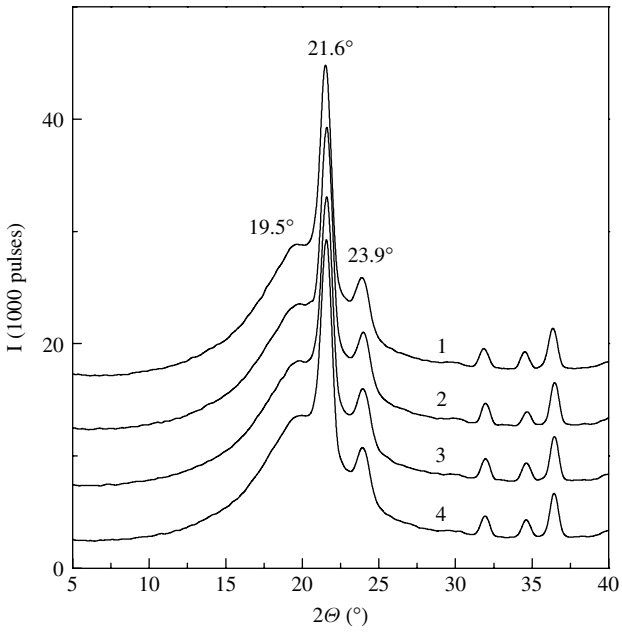

Figure 10. Experimental WAXS curves for unmodified R-LDPE + BR TPE (1) and R-LDPE (PE-*co*-AA)/BR (PB-NCO) with PB-NCO in the BR phase = 1.5 wt% (2), 7.5 wt% (3) and 10 wt% (4). PB-NCO/PE-*co*-AA ratio = 1/1. Beginning from the second curve from the bottom, each next curve was shifted upwards by 5 units.

couples the reactions of the functional groups at the interphase are not effective; the reagents might not have had enough time to react to a sufficient extent.

R-LDPE (PE-*co*-AA) + BR (PB-NCO) TPE was selected for more detailed investigation of the influence of reactive couple content on changes in phase structure, glass transition behavior and degree of crystallinity of polyolefin matrix, as well as on thermal and mechanical properties of TPEs.

STRUCTURE–PROPERTY RELATIONSHIPS IN R-LDPE (PE-*co*-AA) + BR (PB-NCO) TPEs

WAXS diffractograms of unmodified and of all modified TPEs (Fig 10) show two sharp peaks located at the scattering angles of 21.6° and 23.9° (scattering of crystalline phase of polyethylene) as well as a diffuse maximum located at 19.5° (scattering of the amorphous phase of polyethylene).[22,26] As mentioned above, three sharp peaks in the region 31–36° can be attributed to low molecular weight additives used for TPE curing.

The WAXS results show that, in comparison to R-LDPE, the introduction of BR into the R-LDPE matrix leads to changes in the angular positions of the WAXS diffraction peaks of the R-LDPE component. The peaks with angular positions $2\Theta = 21.1°$ and $2\Theta = 23.4°$ move to $2\Theta = 21.6°$ and $2\Theta = 23.9°$, respectively. The positions of the diffraction peaks do not change by introduction and further increase of content of reactive couples in modified TPEs. The respective calculations show that the mean size of microcrystals $\langle D \rangle \approx 11.4–11.5$ nm and the crystal lattice spacing $\langle d \rangle = 0.411$ nm. One can see a certain

increase of the mean size of R-LDPE microcrystals and a decrease of crystal lattice spacing in comparison to R-LDPE.

As mentioned above, the angular positions of diffraction peaks are constant for all TPEs studied, but some changes of intensity of the peaks do occur. This fact is reflected in the change of degree of crystallinity $\langle X \rangle$, and the data are summarized in Table 5. The value of $\langle X \rangle$ represents the overall crystallinity of blend material and can be compared with the theoretical (additive) value, $\langle X \rangle_{add}$, calculated by assuming for R-LDPE its original value of $\langle X \rangle = 27.5$ % and the additivity of components' contribution. The experimental $\langle X \rangle$ is higher than $\langle X \rangle_{add}$, and this implies that the rubber component changes the polyethylene crystallization conditions and that its introduction in crystallizable R-LDPE matrix promotes the phase separation between the crystalline (polyethylene) and amorphous (polyethylene/rubber) phases. It can be seen that the unmodified TPE has the highest value of $\langle X \rangle$. The introduction of reactive couples in TPEs causes destruction of some crystallites. This is reflected in a decrease of onset of melting temperature of crystallites and a depression of the melting temperature T_m –as will be shown below by DSC data. The downward trend of $\langle X \rangle$ can be attributed to reduced phase separation of components in modified TPEs.

The experimental crystallinity values differ from theoretical (additive) ones as a result of interactions between the phases, so that each component affects the microphase structure of the other. This also indicates partial reactively induced compatibilization of BR and R-LDPE. However, the distinctions are not very significant, indicating the existence of regions consisting of individual components in all TPEs. The TPEs modified by PB-NCO + PE-*co*-AA are characterized by higher compatibility of components in comparison to the unmodified TPE and the optimal content of the PB-NCO + PE-*co*-AA modifier corresponds to 7.5 % PB-NCO per BR. These results were confirmed by DSC and DMA data below.

Table 5 shows the experimental values of crystallinity degree calculated from DSC data. The same tendencies are seen as in the WAXS data. Some differences in absolute values occur; the two techniques are known not to give identical results.[21]

Figure 11 shows the C_p (T) plots. Lowering of the melting temperature T_m is observed for all TPEs, and the data are summarized in Table 6. The melting peak corresponds to crystallizable long polyethylene sequences with few chain defects (branching, graftings, etc).[26] Thus, the depression of the melting peak occurs due to increasing defective crystallites content, here mainly because of grafting amide bridges at the thermoplastic/rubber interface. The largest depression of the melting peak is observed for TPE with the content of reactive couple = 7.5 wt%.

The DMA data provide information about relaxation processes.[21] The temperature dependencies of the storage modulus E', the loss modulus E'' and the tan δ are shown in Fig 12. There are significant differences in relaxation behaviour of R-LDPE, BR and TPEs, as well as between modified and unmodified TPEs with the same R-LDPE/BR ratio.

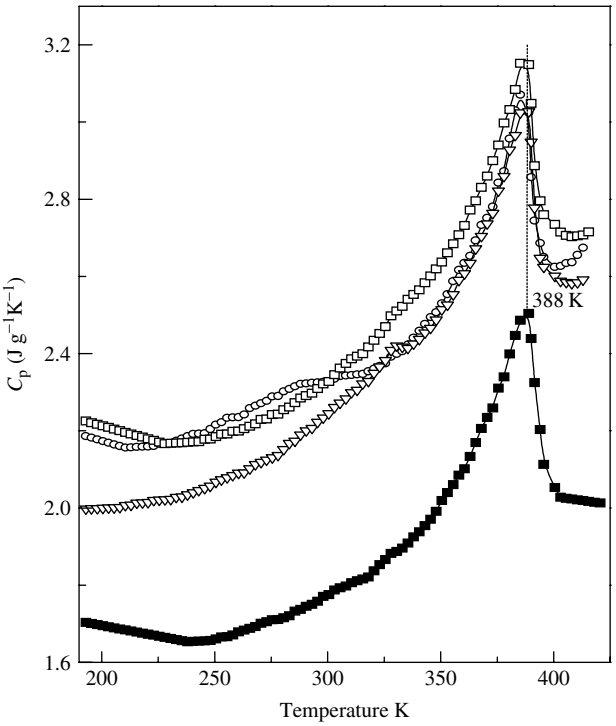

Figure 11. Temperature dependence of the specific heat capacity C_p of TPEs based on: R-LDPE + BR (■);R-LDPE (PE-*co*-AA) + BR (PB-NCO) TPEs with 1.5 wt% (□), 7.5 wt% (○) and 10 wt% (△) of PB-NCO in the BR phase. PB-NCO/PE-*co*-AA ratio = 1/1.

Table 5. The crystalline structure parameters of the TPEs produced

Composition	Mean size of crystallites D (nm)	Crystal lattice spacing d (nm)	WAXS		DSC
			X (%)	X_{add}[a] (%)	X (%)
R-LDPE + BR = 60/40 (unmodified)[b]	11.4	0.411	19.3	16.5	28
R-LDPE (PE-*co*-AA) + BR (PB-NCO):[c]					
PB-NCO = 1.5 wt%	11.4	0.411	18.5	16.4	26
PB-NCO = 7.5 wt%	11.5	0.411	18.0	16.3	17
PB-NCO = 10.0 wt%	11.5	0.411	18.7	16.2	19

[a] $\langle X \rangle_{add}$ is the theoretical (additive) degree of crystallinity: $\langle X \rangle_{add} = X_{(R-LDPE)} \cdot w_i$, where w_i is the polyethylene fraction in TPEs.
[b] R-LDPE/BR = 60/40 (wt%) (ratio kept the same for all samples studied).
[c] NCO/COOH ratio = 1/1.

Table 6. Phase transition temperatures for R-LDPE, BR and TPEs

Composition	DSC		DMA	
			α-relaxation peak temperature[a] (K)	
	T_m (for R-LDPE) (K)	Onset of T_m (K)	BR-rich phase (T_g)	R-LDPE-rich phase (T_{g1})
R-LDPE	389	322	—	353
BR	—	—	253	—
R-LDPE/BR = 60/40 (unmodified)[b]	388	246	258	333
R-LDPE (PE-*co*-AA) + BR (PB-NCO):[c]				
PB-NCO = 1.5 wt%	387	243	266	332
PB-NCO = 7.5 wt%	385	220	262	328
PB-NCO = 10.0 wt%	387	250	265	337

[a] The value taken from the E'' peak.
[b] R-LDPE/BR = 60/40 ratio for all samples.
[c] NCO/COOH ratio = 1/1.

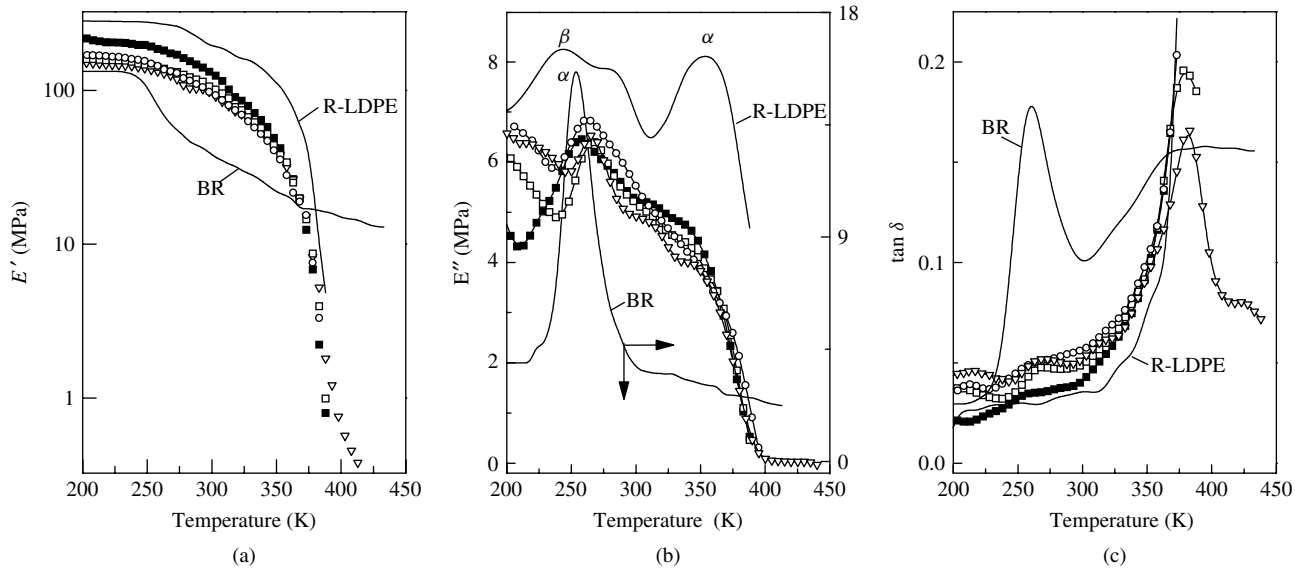

Figure 12. Temperature dependence of (a) storage modulus E', (b) loss modulus E'', and (c) tan δ for R-LDPE, BR and TPEs based on: R-LDPE + BR (■); R-LDPE (PE-*co*-AA) + BR (PB-NCO) TPEs with 1.5 wt% (□), 7.5 wt% (○) and 10 wt% (△) of PB-NCO in BR phase. PB-NCO/PE-*co*-AA ratio = 1/1 e.e.w.

Despite the fact that all TPEs have significant contents of crosslinked chains (see Fig 8), they exhibit thermoplastic properties. The character of E' (T) plots for TPEs at high temperatures (>480 K) is typical for thermoplastic polymers and similar to R-LDPE (see Fig 12(a)). We infer that in all TPEs R-LDPE forms the continuous phase (matrix) while BR is a disperse phase.

Temperature dependencies of E'' (Fig 12(b)) indicate that even virgin BR and R-LDPE have two-phase morphologies. R-LDPE shows two main transitions: an α-transition around 333 K is attributed to motion of $-CH_2$ groups in the crystalline phase during melting and further recrystallization of defective crystallites while the β-transition around 243 K is attributed to relaxation of branched chains in the amorphous phase of LDPE.[27] The high temperature shoulder around 280 K can be assigned to the presence of crosslinked chains in the amorphous phase of R-LDPE (see Table 4).

Cured BR also exhibits two main transitions: the α-relaxation (T_g) around 253 K reflects relaxation of flexible chains of BR while the process with $T_{onset} \approx 300$ K (see Fig 12 (c)) shows relaxation of BR segments limited by intermolecular crosslinking.

The characters of E'' (T) and tan δ (T) plots indicate that in all our TPEs microphase separation of components occurs, resulting in complicated multiphase structures. This conclusion is confirmed by the presence of some overlap transitions in the plots: a low-temperature transition at approximately 210–300 K, a result of a superposition of a strong α-relaxation of BR and the weak β-relaxation of R-LDPE, as well as a high-temperature transition in the region 320–400 K that is a result of superposition of weak relaxation of BR segments limited by intermolecular crosslinking and the strong α-relaxation of R-LDPE. At temperatures above approximately 380 K the melting of crystallizable long polyethylene

sequences with a low number of chain defects begins.

The temperature positions of α-relaxation peaks taken from corresponding peaks of the E'' (T) plot (see Fig 12(b)) of the BR-rich and R-LDPE-rich phases are listed in Table 6. Clearly α-relaxation peaks of BR and R-LDPE are shifted towards one another in modified TPEs. This can be explained by the interaction between BR and R-LDPE phases due to the formation of the interface layer mainly based on PB-NCO + PE-*co*-AA grafting from rubber and polyethylene phases, respectively.

The relaxation processes in amorphous phases are hampered by the presence of R-LDPE crystallites.[3] However, Fig 12 (c)) indicates some increase of intensity of relaxation transitions at 230–295 K for modified TPEs in comparison to unmodified TPE or pure R-LDPE. This implies higher chain mobility in amorphous phases at the expense of the crystalline phase of R-LDPE. These results are supported by both WAXS and DSC data.

Thus, DMA results show that the TPEs are multiphase systems with at least one crystalline and two amorphous phases of individual components and regions of mixed compositions. We presume that the R-LDPE crystalline phase consists of microregions formed by 'perfect' crystallites and by 'defective' crystallites, while the R-LDPE amorphous phase consists of microregions formed by crosslinked chains and by branched chains. The BR amorphous phase consists of microregions formed by crosslinked segments and also one formed by flexible linear BR chains. The mixed microphase consists of both the components grafted by reactive compatibilizers. Thus, the final properties of TPEs are determined by the heterogeneity of the individual components, as well as by the heterogeneity caused by the thermodynamic immiscibility of the components. The degree of compatibilization is affected to a large extent by the grafting reaction of PB-NCO + PE-*co*-AA reactive compatibilizer and by the formation of the extensive interfacial layer that leads to improved interfacial adhesion between rubber and polyethylene phases.

CONCLUSIONS

Needless to say, a broader perspective of the present paper is protection of the environment from the fast growth of waste originating from synthetic polymeric materials. Several options exist here. One is the combination of synthetic polymers with natural ones, such as the work of Albano and her coworkers on mixing high density PE (HDPE) and polypropylene with wood flour and sisal fibers.[28,29] Somewhat related is regeneration of cellulose in controlled media resulting in environmentally friendly cellulose fibers.[30] A different approach is the use of synthetic polymers which can be degraded by natural means, such as the work of Lopez and her colleagues on biodegradation of copolymers of PE and vinyl alcohol by a fungus.[31] A further different route is the one we have followed: recycling combined with compatibilization. There is a variety of compatibilizers, such as an olefinic ionomer applied to an HDPE + polyurethane system.[32] We achieved compatibilization by relatively simple means. While our resulting phase structures are complicated, the objective of protection of the environment is achieved along with an improvement of mechanical properties.

ACKNOWLEDGEMENTS

The authors are grateful to the Robert A Welch Foundation, Houston (Grant B-1203), the European Union, Brussels (INCO-Copernicus project–Contract No: ICA2-CT-2001-10003) and to the US Department of Commerce, Washington, DC (SABIT Program) for partial financial support of this work. Constructive comments of the referees on the manuscript of this paper are appreciated.

REFERENCES

1 Adhikari B, De D and Maiti S, *Prog Polym Sci* **25**:909 (2000).
2 George J, Varughese KT and Thomas S, *Polymer* **41**:1507 (2000).
3 Nevatia P, Banerjee TS, Dutta B, Jha A, Naskar AK and Bhowmick AK, *J Appl Polym Sci* **83**:2035 (2002).
4 Karger-Kocsis J, in *Polymer Blends and Alloys*, ed by Shonaike GO and Simon GP, Marcel Dekker, New York, pp 125–153 (1999).
5 Michael H, Scholz H and Menning G, *Kautschuk und Gummi*, **5**:510 (1999).
6 Bhattacharya SN and Sbarski I, *Plast Rubber Compos Process Appl* **27**:317 (1998).
7 Yang Y, Chiba T, Saito H and Inoue T, *Polymer* **39**:3365 (1998).
8 Spontak RJ and Patel NP, *Curr Opin Colloid Interface Sci* **5**:334 (2000).
9 Kim Y, Cho W-J and Ha C-S, *Polym Eng Sci* **35**:1592 (1995).
10 Fainleib A, Grigoryeva O, Starostenko O and Brostow W, *Proc Halle Internat Conf Polym Mater* 159 (2002).
11 Grigoryeva O, *Chem Listy Symp* 237 (2002).
12 Fainleib A, Grigoryeva O, Starostenko O, Brovko A and Vilensky V, *Proc IUPAC World Polymer Congress MACRO 2002–Beijing*, 1000 (2002).
13 Radusch H-J, Corley B and Hai LH, *Proc 14th Bratislava Internat Conf Modified Polymers*, 27 (2000).
14 Corley B and Radusch H-J, *J Macromol Sci, Phys* **B37**:265 (1998).
15 Orr, CA, Cernohous JJ, Guegan P, Hirao A, Jeon HK and Macosko CW, *Polymer* **42**:8171 (2001).
16 Bray T, Damiris S, Grace A, Moad G, O'Shea M, Rizzardo E and Diepen GV, *Macromol Symp* **129**:109 (1998).
17 Fainleib A, Grigoryeva O, Starostenko O, Danilenko I and Bardash L, *Macromol Symp* **202**:117 (2003).
18 Fainleib A, Grigoryeva O and Starostenko O, *Proc IUPAC World Polymer Congress MACRO 2002–Beijing*, 998 (2002).
19 Campbell D and White JR, *Polymer Characterization*, Chapman & Hall, London (1989).
20 Matthews JL, Peiser HS and Richards RB, *Acta Crystallogr* **2**:85 (1949).
21 Menard KP, *Dynamic Mechanical Analysis—An Introduction*, CRC Press, Boca Raton, FL (1999); Menard KP, Ch 8 in *Performance of Plastics*, ed by Brostow W, Hanser, Munich-Cincinnati (2000).
22 Krimm S and Tobolsky A, *J Polym Sci* **7**:57 (1951).

23 Hermans PH and Weidinger A, *Makromol Chem* **44–46**:24 (1961).
24 Radonjic G and Gubeljak N, *Macromol Mater Eng* **287**:122 (2002).
25 Mark JE editor, *Physical Properties of Polymers Handbook*, American Institute of Physics Press, Woodbury, NY (1996).
26 Greco R, Musto P, Riva F and Maglio G, *J Appl Poly Sci* **37**:789 (1989).
27 Akovali G and Torun TT, *Polym Int* **42**:307 (1997).
28 Albano C, Ichazo M, González J, Delgado M and Poleo R, *Mater Res Innovat* **4**:284 (2001).
29 Reyes J, Albano C, Davidson E, Poleo R, González J, Ichazo M and Chipara M, *Mater Res Innovat* **4**:294 (2001).
30 Kreze T, Strnad S, Stana-Kleinschek K and Ribitsch V, *Mater Res Innovat* **4**:107 (2001).
31 Mejia G, Lopez BL and Sierra L, *Mater Res Innovat* **4**:148 (2001).
32 Papadopoulou CP and Kalfoglou NK, *Polymer* **40**:905 (1999).